

# Reflection symmetric second-order topological insulators and superconductors

Josias Langbehn, Yang Peng, Luka Trifunovic, Felix von Oppen, and Piet W. Brouwer<sup>1</sup>

<sup>1</sup>*Dahlem Center for Complex Quantum Systems and Physics Department,  
Freie Universität Berlin, Arnimallee 14, 14195 Berlin, Germany*

(Dated: October 31, 2017)

Second-order topological insulators are crystalline insulators with a gapped bulk and gapped crystalline boundaries, but topologically protected gapless states at the intersection of two boundaries. Without further spatial symmetries, five of the ten Altland-Zirnbauer symmetry classes allow for the existence of such second-order topological insulators in two and three dimensions. We show that reflection symmetry can be employed to systematically generate examples of second-order topological insulators and superconductors, although the topologically protected states at corners (in two dimensions) or at crystal edges (in three dimensions) continue to exist if reflection symmetry is broken. A three-dimensional second-order topological insulator with broken time-reversal symmetry shows a Hall conductance quantized in units of  $e^2/h$ .

*Introduction.*—After the discovery of topological insulators and superconductors and their classification for the ten Altland-Zirnbauer symmetry classes [1–3], the concept of nontrivial topological band structures has been extended to materials in which the crystal structure is essential for the protection of topological phases [4]. This includes weak topological insulators [5], which rely on the discrete translation symmetry of the crystal lattice, and topological crystalline insulators [6], for which other crystal symmetries are invoked to protect a topological phase. Whereas the original strong topological insulators always have topologically protected boundary states, weak topological insulators or topological crystalline insulators have protected boundary states for selected surfaces/edges only.

In a recent publication, Schindler *et al.* [7] proposed another extension of the topological insulator (TI) family: a higher-order topological insulator. Being crystalline insulators, these have well-defined faces and well-defined edges or corners at the intersections between the faces. An  $n$ th order topological insulator has topologically protected gapless states at the intersection of  $n$  crystal faces, but is gapped otherwise [7]. For example, a second-order topological insulator in two dimensions ( $d = 2$ ) has zero-energy states at corners, but a gapped bulk and no gapless edge states. Earlier examples of higher-order topological insulators and superconductors *avant la lettre* appeared in works by Benalcazar *et al.* [8–10] (see also [11, 12]), who considered insulators and superconductors with protected corner states in  $d = 2$  and  $d = 3$  [13]. Sitte *et al.* showed that a three-dimensional topological insulator in a magnetic field of generic direction also acquires the characteristics of a second-order topological Chern insulator, with chiral states moving along the sample edges [14].

Since a second-order TI has a topologically trivial  $d$ -dimensional bulk, from a topological point of view its boundaries are essentially stand-alone ( $d - 1$ -

dimensional insulators, so that topologically protected states at corners (for  $d = 2$ ) or edges (for  $d = 3$ ) arise naturally as “domain walls” at the intersection of two boundaries if these are in different topological classes [1, 15, 16]. Similarly, the classification of  $n$ th order TIs derives from that of TIs in  $d + 1 - n$  dimensions, *i.e.*, the same classification of codimension  $n$  topological defects [17] (see [18] for a scattering-approach based classification of  $n$ th order TIs). Note that, unlike for strong topological insulators and superconductors, which have protected states at all boundaries,  $n$ th-order topological insulators and superconductors have topologically protected states at the intersection of  $n$  boundaries *only* if (some of) these boundaries are in different topological classes; they do not necessarily have protected states at *all* intersections of  $n$  boundaries.

Apart from their role in stabilizing well-defined crystal faces, crystalline symmetries are not required for the protection of higher-order TIs. However, crystal symmetries can be a key to ensure that a natural surface termination — *i.e.*, a surface termination that respects the crystal symmetries — automatically leads to a nontrivial higher-order topological phase. For example, Benalcazar *et al.* employed a combination of multiple reflection symmetries [9], whereas Schindler *et al.* considered  $C_4\mathcal{T}$  symmetry, the product of a  $\pi/2$  rotation and time reversal, as well as a model with reflection symmetry [7].

In this letter, we show that a single mirror symmetry is sufficient to construct models for second-order topological insulators and superconductors in  $d = 2$  and  $d = 3$  for all five Altland-Zirnbauer classes for which second-order topological insulators are allowed. Reflection-symmetric topological crystalline insulators were the first to be realized experimentally [16, 19, 20]. A complete classification of reflection-symmetric topological insulators and superconductors exists for all ten Altland-Zirnbauer classes [21, 23, 24, 52], and our construction makes

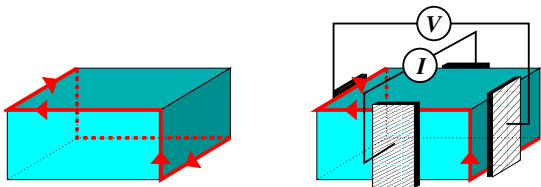


FIG. 1. A generic reflection-symmetric second-order topological insulator has chiral edge states winding around the crystal (left). If current and voltage contacts cover at most two neighboring edges, such a sample shows edge transport and, consequently, a quantized Hall effect in three dimensions (right).

use of this classification. Since the second-order topological phase does not *require* the reflection symmetry for its existence — see our general remarks above and our detailed discussion below —, in practice an approximate reflection symmetry may well be sufficient, which significantly enhances the prospects of an experimental realization.

An (approximately) reflection-symmetric three-dimensional second-order topological insulator with broken time-reversal symmetry has chiral edge states winding around the sample if none of its crystal faces is reflection symmetric, see Fig. 1(a). Despite being three-dimensional, such crystals show a Hall effect with Hall *conductance* quantized in units of  $e^2/h$ , if current and voltage probes are attached such that they touch a single sample edge or two neighboring edges, see Fig. 1(b) [14]. Such a quantized Hall effect for a three-dimensional crystal is different from the “three-dimensional quantized Hall effect”, which involves a topologically nontrivial bulk state and a quantized Hall *conductivity* [25–29]. Similarly, a reflection- and time-reversal-symmetric three-dimensional second-order topological insulator has a one-dimensional helical edge state winding around the crystal, corresponding to a quantized spin Hall effect in three dimensions. The experimental detection of such a quantized (spin) Hall effect should be an unambiguous experimental signature of a second-order TI.

*Second-order topological insulators with reflection symmetry.*—Since corners and edges follow the classification of one-dimensional and two-dimensional topological insulators and superconductors, second-order topological insulators with protected zero-energy corner states or with gapless edge states can exist for selected Altland-Zirnbauer classes only, see Table I. We now provide a systematic method to construct examples of second-order topological insulators in all five nontrivial Altland-Zirnbauer classes, using a single reflection symmetry  $\mathcal{R}$  to ensure the presence of topologically protected corner or edge states.

For each allowed Altland-Zirnbauer class, the construction requires (i) one or more pairs of crystal faces that are mapped onto each other by reflection and (ii) a reflection-symmetric topological crystalline phase which becomes trivial if the reflection symmetry is broken. The nontrivial topology of the corresponding Altland-Zirnbauer class in  $d - 1$  dimensions guarantees that the reflection-symmetry-breaking mass term that gaps out any boundary states existing in the presence of reflection symmetry is unique. Since this mass term must be *odd* under reflection, the two surfaces listed under (i) must be in different topological classes, ensuring the existence of zero energy (gapless) states at at least two corners (edges). Table I lists the reflection-symmetric phases that meet these criteria. We emphasize again that the reflection symmetry is used to *construct* the second-order topological insulator; it is itself not essential for the existence of zero-energy corner states (for  $d = 2$ ) or gapless edge states (for  $d = 3$ ). The corner states (edge states) are robust against a reflection-symmetry breaking perturbation, as long as the bulk and edge (surface) gaps are not closed [30].

Below we discuss three examples in detail: A two-dimensional second-order topological superconductor with Majorana corner states (class D), a three-dimensional second-order topological insulator with chiral edge states (class A), and a three-dimensional second-order topological insulator with helical edge states (class AII). In all cases we take reflection to map the momentum component  $k_1$  into  $-k_1$ , leaving the other momentum components unchanged.

*Second-order topological superconductor: class D.*—For a superconductor with broken time-reversal and spin-rotation symmetry, particle-hole symmetry  $\mathcal{P}$  is the only relevant symmetry operation. Without loss of generality we may represent  $\mathcal{P}$  by complex conjugation  $K$  by working in a Majorana basis and the reflection operation by the Pauli matrix  $\sigma_1$  in an orbital subspace, so that the Hamiltonian  $H(k_1, k_2)$  satisfies

$$\begin{aligned} H(k_1, k_2) &= -H^*(-k_1, -k_2) \\ &= \sigma_1 H(-k_1, k_2) \sigma_1. \end{aligned} \quad (1)$$

Without reflection symmetry, class D in two dimensions has a  $\mathbb{Z}$  classification, where the integer topological number counts the number of chiral Majorana edge modes [31, 32]. Chiral Majorana modes are incompatible with reflection symmetry. Instead, with reflection symmetry a  $\mathbb{Z}_2$  topological structure remains [21, 23, 52], counting the parity of the number of helical (*i.e.*, counter-propagating) Majorana edge modes. A minimal reflection-symmetric nontrivial gapless edge state at a reflection-symmetric

Cartan	$\mathcal{T}$	$\mathcal{P}$	$\mathcal{C}$		$d = 2$		$d = 3$
A	0	0	0	0	—	$\mathbb{Z}$	$\mathcal{R}$
AIII	0	0	1	$\mathbb{Z}$	$\mathcal{R}_+$	0	—
AI	1	0	0	0	—	0	—
BDI	1	1	1	$\mathbb{Z}$	$\mathcal{R}_{++}$	0	—
D	0	1	0	$\mathbb{Z}_2$	$\mathcal{R}_+$	$\mathbb{Z}$	$\mathcal{R}_+$
DIII	-1	1	1	$\mathbb{Z}_2$	$\mathcal{R}_{++}, \mathcal{R}_{--}$ $\mathcal{R}_{-+}$	$\mathbb{Z}_2$	$\mathcal{R}_{++}, \mathcal{R}_{-+}$
AII	-1	0	0	0	—	$\mathbb{Z}_2$	$\mathcal{R}_+, \mathcal{R}_-$
CII	-1	-1	1	$\mathbb{Z}$	$\mathcal{R}_{++}, \mathcal{R}_{--}$	0	—
C	0	-1	0	0	—	$\mathbb{Z}$	$\mathcal{R}_+, \mathcal{R}_-$
CI	1	-1	1	0	—	0	—

TABLE I. The ten Altland-Zirnbauer classes are defined according to the presence or absence of time-reversal ( $\mathcal{T}$ ), particle-hole ( $\mathcal{P}$ ), and chiral symmetry ( $\mathcal{C}$ ). A nonzero entry indicates the square of the antiunitary symmetry operations  $\mathcal{T}$  or  $\mathcal{P}$ . Two-dimensional and three-dimensional reflection-symmetric topological crystalline phases that can be used for the construction of second-order topological insulator/superconductor phases are listed in the right two columns, together with the corresponding topological classification. The symbols  $\mathcal{R}_{\sigma\mathcal{T}}$ ,  $\mathcal{R}_{\sigma\mathcal{P}}$ ,  $\mathcal{R}_{\sigma\mathcal{C}}$ , and  $\mathcal{R}_{\sigma\mathcal{T},\sigma\mathcal{P}}$  refer to a reflection operator that squares to one and commutes ( $\sigma = +$ ) or anticommutes ( $\sigma = -$ ) with  $\mathcal{T}$ ,  $\mathcal{P}$ , or  $\mathcal{C}$ .

edge has edge Hamiltonian  $H_{\text{edge}} = vk_1\sigma_3$ , with  $v$  the velocity, which is a trivial edge in the absence of  $\mathcal{R}$ . Indeed, upon breaking reflection symmetry,  $H_{\text{edge}}$  is gapped out by a unique mass term  $m\sigma_2$ . An explicit model realizing this scenario is given by the four-band tight-binding Hamiltonian,

$$H = (M - \cos k_1 - \cos k_2)\tau_2 + \tau_1\sigma_3 \sin k_1 + \tau_3 \sin k_2 + \lambda\tau_2\sigma_1, \quad (2)$$

with  $0 < |M| < 2$  and  $\lambda$  numerically small. The physical implementation would require stacking two  $p_x \pm ip_y$  superconductors [33] with opposite chirality and coupling them in such a way to gap-out edge-modes at non-reflection symmetric edges.

Computing the spectrum of low-lying excitations for a rectangular crystal with edges at 45 degrees with respect to the symmetry axis we find a zero-energy state well separated from higher-lying excitations by a gap. The wavefunction of the zero-energy states is localized near the two sample corners where the reflection-related edges meet, as shown in Fig. 7(a) and (b) for two different arrangements of the reflection line with respect to the corner of the crystal. The localized zero mode persists if the crystal is rotated, such that there are no longer any reflection-related edges [Fig. 7(c)].

*Second-order topological insulator in three dimensions: class A.*—In three dimensions the presence of reflection symmetry allows for a topological crystalline phase with an integer “mirror Chern number” enumerating gapless surface states at reflection-

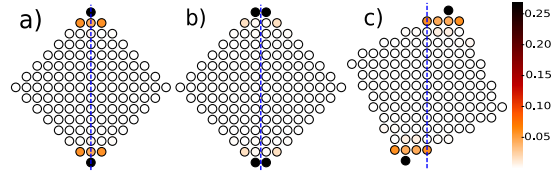


FIG. 2. Weight of the zero-energy wavefunction for the Hamiltonian (2) with  $M = 0.9$  and  $\lambda = -0.25$  for three orientations of the crystal lattice. The reflection line is shown dashed.

symmetric surfaces [21, 23, 34, 52]. Using  $\sigma_1$  to represent the reflection operation, such surface states have Hamiltonian  $H_{\text{surface}} = v_1k_1\sigma_3 + v_2k_2\sigma_1$ . The unique mass term gapping out such surface states is  $m\sigma_2$ , which is odd under reflection. Explicitly, one may consider the four-band Hamiltonian

$$H = (M - \cos k_1 - \cos k_2 - \cos k_3)\tau_2\sigma_1 + \sigma_3 \sin k_1 + \tau_1\sigma_1 \sin k_2 + \tau_3\sigma_1 \sin k_3 + B\tau_2. \quad (3)$$

where  $\sigma$  and  $\tau$  are Pauli matrices in the space spanned by the unit-cell orbitals two of which are even (odd) under reflection. For  $1 < M < 3$  and  $B$  numerically small this Hamiltonian describes a three-dimensional topological insulator with a reflection-symmetric time-reversal-symmetry-breaking term. To see how the bulk  $B\tau_2$  term gives rise to the  $\sigma_2$  term at the non-reflection symmetric facet, we first note that the details of the boundary do not have influence of the choice of the  $B$ -term. Thus to obtain facet-Hamiltonian for one of the  $yz$ -facets it is sufficient to use low-energy expansion of the Hamiltonian (3) and model the boundary by the mass  $M$  domain-wall along  $x$ -direction. This way we immediately conclude that the projector onto the  $yz$ -facet Hamiltonian is given by  $\tau_2\sigma_2 = \pm 1$ , therefore the term  $B\tau_2$  acts like  $\sim \sigma_2$  within the surface subspace (the proportionality factor does depends on the interface details).

Figure 3(b) shows the band structure of a rectangular crystal with surfaces in the (110) and (1 $\bar{1}$ 0) direction, and periodic boundary conditions in the  $k_3$  direction. The two gapless chiral modes running in the positive and negative  $k_3$  direction are located at the intersection of the (110) and (1 $\bar{1}$ 0) surfaces related by  $\mathcal{R}$ , see Fig. 3(a). We verified that the chiral edge states persist if the crystal orientation is rotated by an angle less than 45 degrees and migrates to the other pair of edges for larger rotation angles. Figure 3(c) shows the support of a chiral edge state for the above model Hamiltonian for a cubic sample randomly oriented with respect to the reflection plane (so that none of the facets are reflection symmetric).

*Second-order topological insulator in three dimen-*

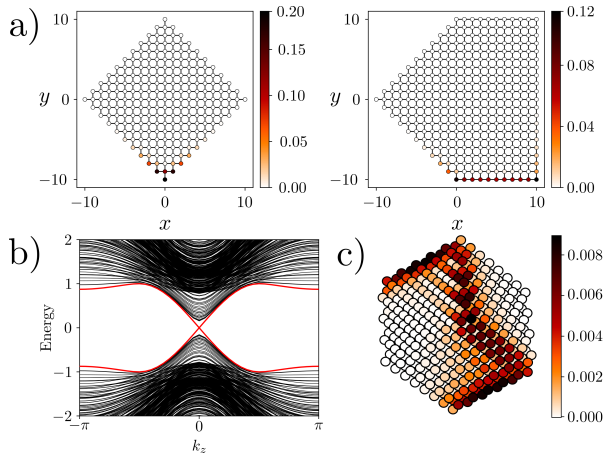


FIG. 3. (a) The crystal shape and the spatial profile of one of the in-gap states. Left: when the two surfaces meet at the reflection plane under a sharp angle, the in-gap state is well localized; right: one surface is perpendicular to the reflection plane, the in-gap state becomes completely delocalized on that surface. (b) Band structure of a rectangular crystal with periodic boundary conditions in the  $k_3$  direction, for the model (3) with parameters  $M = 2$ ,  $B = 0.2$ . (c) Weight of the zero-energy chiral edge states for a finite lattice with generic orientation with respect to the reflection plane.

*sions: class AII.*—We represent the time-reversal and reflection operations by  $\sigma_2 K$  and  $\sigma_1$ , respectively, so that  $H(k_1, k_2, k_3)$  satisfies

$$\begin{aligned} H(k_1, k_2, k_3) &= \sigma_2 H(-k_1, -k_2, -k_3)^* \sigma_2 \\ &= \sigma_1 H(-k_1, k_2, k_3) \sigma_1. \end{aligned} \quad (4)$$

Hamiltonians with this symmetry have a  $\mathbb{Z}$  topological classification [21, 23, 34, 52] which enumerates the number of surface states with Dirac-like dispersion  $H_{\text{surface}} = v_1 k_1 \sigma_3 + v_2 k_2 \sigma_1$  at reflection-symmetric surfaces. The unique  $\mathcal{R}$ -breaking mass term that gaps out such a pair of surface states is  $m \sigma_2 \tau_2$ , where  $\tau_2$  is an additional Pauli matrix. (A single surface Dirac cone is protected by time-reversal symmetry.) Since this mass term is odd under reflection, we expect an integer number of one-dimensional helical states at the intersection of two surfaces related by  $\mathcal{R}$ . An even number of helical states is unstable, however, to a local perturbation at the edge and can be gapped out without closing the gaps in the sample bulk or at the surfaces, consistent with the  $\mathbb{Z}_2$  classification in Table I. (At this point our classification differs from that of Ref. [7], which does not allow for reflection-symmetry breaking perturbations at the crystal edge, thus arriving at a  $\mathbb{Z}$  [24] classification.) As a specific example, we

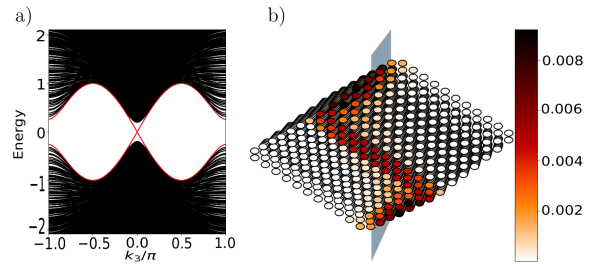


FIG. 4. (a) Band structure of a rectangular crystal with periodic boundary conditions in the  $k_3$  direction, for the model (5) with parameters  $M = 2$ ,  $B = 0.8$ . The crystal shape is the same as in Fig. 3. (b) Weight of the zero-energy chiral edge states for a finite lattice with generic orientation with respect to the reflection plane.

consider the eight-band Hamiltonian

$$\begin{aligned} H &= [(M - \cos k_1 - \cos k_2 - \cos k_3) \tau_2 \sigma_1 \\ &\quad + \sigma_3 \sin k_1 + \tau_1 \sigma_1 \sin k_2 + \tau_3 \sigma_1 \sin k_3] \rho_0 \\ &\quad + B \tau_2 \rho_2, \end{aligned} \quad (5)$$

where  $\rho_{0,1,2}$  are an additional set of Pauli matrices,  $1 < M < 3$ , and  $B$  numerically small. One-dimensional band structure and weights for zero-energy states are shown in Fig. 4 for the same geometry as in the previous example.

*Conclusion.*—Although second-order topological insulators and superconductors can exist without a topological crystalline bulk phase, the existence of (approximate) crystalline symmetries can help in the construction of models or in the identification of materials that realize these phases. For reflection-symmetric topological crystalline insulators, the published literature has focused on reflection-symmetric surfaces, because these surfaces harbor topologically protected surface states [4, 16, 19, 20, 34]. We have shown that there is a good reason to look at crystals with arbitrarily oriented surfaces, because such crystals are good candidates for second-order TIs. Whereas the surface states of reflection-symmetric topological crystalline insulators are vulnerable to even weak perturbations that break the reflection symmetry, the associated edge states are robust and persist as long as surface and bulk gaps remain open. Combined with the unique prospect of isolated Majorana bound states (for two-dimensional second-order topological superconductors) or one-dimensional chiral modes and a quantized Hall effect (for three-dimensional second-order TIs), higher-order TIs are a promising addition to the topological materials family. Very recently, some early experimental realizations of second-order topological insulators appeared [35–38], where the Ref. [35] uses the bismuth nanowire which was previously shown to support edge states [39].

*Acknowledgments.*—This work was motivated by a colloquium on  $C_4\mathcal{T}$ -symmetric higher-order topological insulators by Titus Neupert at FU Berlin and subsequent discussions. We also thank Andrei Bernevig and Max Geier for discussions. We gratefully acknowledge support by projects A03 and C02 of the CRC-TR 183 and by the priority programme SPP 1666 of the German Science Foundation (DFG).

*Note added.*—After completion of this manuscript, we became aware of related works by Ref. [40, 41].

- 
- [1] M. Z. Hasan and C. L. Kane, *Rev. Mod. Phys.* **82**, 3045 (2010).
- [2] B. A. Bernevig and T. L. Hughes, *Topological Insulators and Topological Superconductors* (Princeton University Press, 2013).
- [3] X.-L. Qi and S.-C. Zhang, *Rev. Mod. Phys.* **83**, 1057 (2011).
- [4] C.-K. Chiu, J. C. Y. Teo, A. P. Schnyder, and S. Ryu, *Rev. Mod. Phys.* **88**, 035005 (2016).
- [5] L. Fu, C. L. Kane, and E. J. Mele, *Phys. Rev. Lett.* **98**, 106803 (2007).
- [6] L. Fu, *Phys. Rev. Lett.* **106**, 106802 (2011).
- [7] F. Schindler, A. M. Cook, M. G. Vergniory, Z. Wang, S. S. Parkin, B. A. Bernevig, and T. Neupert, arXiv:1708.03636 (2017).
- [8] W. A. Benalcazar, J. C. Y. Teo, and T. L. Hughes, *Phys. Rev. B* **89**, 224503 (2014).
- [9] W. A. Benalcazar, B. A. Bernevig, and T. L. Hughes, arXiv:1611.07987 (2016).
- [10] W. A. Benalcazar, B. A. Bernevig, and T. L. Hughes, ArXiv e-prints (2017), arXiv:1708.04230 [cond-mat.mes-hall].
- [11] Y. Peng, Y. Bao, and F. von Oppen, *Phys. Rev. B* **95**, 235143 (2017).
- [12] F. Zhang, C. L. Kane, and E. J. Mele, *Phys. Rev. Lett.* **110**, 046404 (2013).
- [13] Reference 8 views the corner of a three-dimensional lattice as a disclination of the surface. In contrast, the corner states of a two-dimensional second-order TI exist as the corners of a “flat” surface.
- [14] M. Sitte, A. Rosch, E. Altman, and L. Fritz, *Phys. Rev. Lett.* **108**, 126807 (2012).
- [15] R. Jackiw and C. Rebbi, *Phys. Rev. D* **13**, 3398 (1976).
- [16] T. H. Hsieh, H. Lin, J. Liu, W. Duan, A. Bansil, and L. Fu, *Nat. Comm.* **3**, 982 (2012).
- [17] J. C. Y. Teo and C. L. Kane, *Phys. Rev. B* **82**, 115120 (2010).
- [18] See Supplementary Material for a scattering-approach based classification of  $n$ th order TIs, which includes Refs. [9, 15, 21, 23, 24, 42–52].
- [19] Y. Tanaka, Z. Ren, T. Sato, K. Nakayama, S. Souma, T. Takahashi, K. Segawa, and Y. Ando, *Nat. Phys.* **8**, 800 (2012).
- [20] S.-Y. Xu, C. Liu, N. Alidoust, M. Neupane, D. Qian, I. Belopolski, J. D. Denlinger, Y. Wang, H. Lin, L. A. Wray, G. Landolt, B. Slomski, J. H. Dil,  
A. Marcinkova, E. Morosan, Q. Gibson, R. Sankar, F. C. Chou, R. J. Cava, A. Bansil, and M. Z. Hasan, *Nature Comm.* **3**, 1192 (2012).
- [21] C.-K. Chiu, H. Yao, and S. Ryu, *Phys. Rev. B* **88**, 075142 (2013).
- [52] T. Morimoto and A. Furusaki, *Phys. Rev. B* **88**, 125129 (2013).
- [23] K. Shiozaki and M. Sato, *Phys. Rev. B* **90**, 165114 (2014).
- [24] L. Trifunovic and P. W. Brouwer, arXiv:1707.06306 (2017).
- [25] B. I. Halperin, *Jpn. J. Appl. Phys.* **26**, 1913 (1987).
- [26] G. Montambaux and M. Kohmoto, *Phys. Rev. B* **41**, 11417 (1990).
- [27] J. T. Chalker and A. Dohmen, *Phys. Rev. Lett.* **75**, 4496 (1995).
- [28] M. Koshino, H. Aoki, K. Kuroki, S. Kagoshima, and T. Osada, *Phys. Rev. Lett.* **86**, 1062 (2001).
- [29] M. Koshino, H. Aoki, T. Osada, K. Kuroki, and S. Kagoshima, *Phys. Rev. B* **65**, 045310 (2002).
- [30] In principle, since the corners (edges) featured in the above construction may themselves be reflection symmetric, the reflection symmetry may allow for additional states. These, however, can be gapped out by any weak perturbation that breaks the reflection symmetry.
- [31] G. E. Volovik, *Zh. Eksp. Teor. Fiz.* **94**, 123 (1988), [*Sov. Phys. JETP* **67**, 1804 (1988)].
- [32] N. Read and D. Green, *Phys. Rev. B* **61**, 10267 (2000).
- [33] P. A. Lee, ArXiv e-prints (2009), arXiv:0907.2681 [cond-mat.str-el].
- [34] J. C. Y. Teo, L. Fu, and C. L. Kane, *Phys. Rev. B* **78**, 045426 (2008).
- [35] A. Murani, A. Kasumov, S. Sengupta, Y. A. Kasumov, V. T. Volkov, I. I. Khodos, F. Brisset, R. Delagrè, A. Chepelianskii, R. Deblock, H. Bouchiat, and S. Guéron, *Nat. Comm.* **8**, 15941 (2017).
- [36] M. Serra-Garcia, V. Peri, R. Süssstrunk, O. R. Bilal, T. Larsen, L. G. Villanueva, and S. D. Huber, ArXiv e-prints (2017), arXiv:1708.05015 [cond-mat.mtrl-sci].
- [37] C. W. Peterson, W. A. Benalcazar, T. L. Hughes, and G. Bahl, ArXiv e-prints (2017), arXiv:1710.03231 [cond-mat.mes-hall].
- [38] S. Imhof, C. Berger, F. Bayer, J. Brehm, L. Molenkamp, T. Kiessling, F. Schindler, C. H. Lee, M. Greiter, T. Neupert, and R. Thomale, ArXiv e-prints (2017), arXiv:1708.03647 [cond-mat.mes-hall].
- [39] O. Deb, A. Soori, and D. Sen, *J. Phys.: Condens. Matter* **26**, 315009 (2014).
- [40] Z. Song, Z. Fang, and C. Fang, arXiv:1708.02952 (2017).
- [41] W. A. Benalcazar, B. A. Bernevig, and T. L. Hughes, arXiv:1708.04230 (2017).
- [42] R. B. Laughlin, *Phys. Rev. B* **23**, 5632 (1981).
- [43] S. H. Simon, *Phys. Rev. B* **61**, R16327 (2000).
- [44] D. Meidan, T. Micklitz, and P. W. Brouwer, *Phys. Rev. B* **82**, 161303 (2010).
- [45] D. Meidan, T. Micklitz, and P. W. Brouwer, *Phys. Rev. B* **84**, 195410 (2011).
- [46] I. C. Fulga, F. Hassler, A. R. Akhmerov, and C. W. J. Beenakker, *Phys. Rev. B* **83**, 155429

- (2011).
- [47] I. C. Fulga, F. Hassler, and A. R. Akhmerov, Phys. Rev. B **85**, 165409 (2012).
- [48] L. Fu and C. L. Kane, Phys. Rev. B **74**, 195312 (2006).
- [49] F. Merz and J. T. Chalker, Phys. Rev. B **65**, 054425 (2002).
- [50] A. R. Akhmerov, J. P. Dahlhaus, F. Hassler, M. Wimmer, and C. W. J. Beenakker, Phys. Rev. Lett. **106**, 057001 (2011).
- [51] A. Lau, J. van den Brink, and C. Ortix, Phys. Rev. B **94**, 165164 (2016).
- [52] T. Morimoto and A. Furusaki, Phys. Rev. B **88**, 125129 (2013).

---

## SUPPLEMENTAL MATERIAL

### CLASSIFICATION BASED ON SCATTERING THEORY

A variation of Laughlin’s famous argument for a quantized Hall conductivity [42], can be used to classify corners, edges, etc. of  $n$ th order topological insulators in  $d$  dimensions in terms of their reflection matrices. The classification closely follows the existing reflection-matrix-based classification procedure for boundary states of topological insulators in  $d + 1 - n$  dimensions [43–48]. We first illustrate the reflection-matrix-based classification procedure for second-order TIs in two dimensions, and then discuss the generalization to higher orders and higher dimensions.

For the classification of the corners of a two-dimensional crystal we attach a one-dimensional lead to each corner, as shown in Fig. 5 (left). Each lead has the number  $g$  of degrees of freedom required for the corresponding Altland-Zirnbauer class. (For example,  $g = 2$  for a spinless Bogoliubov-de Gennes Hamiltonian, corresponding to particle and hole degrees of freedom.) Since bulk and edges of the two-dimensional crystal are gapped, each lead is described by a unitary reflection matrix  $r_j$ . There is a topologically protected (zero-energy) corner state at the  $j$ th corner if and only if  $r_j$  is “topologically nontrivial”, where the precise meaning of “topologically nontrivial” depends on the Altland-Zirnbauer class under consideration [46]. For example, for class D the topological number is  $\text{sign det } r_j$  [49, 50]. The same classification procedure can be used for the two ends of a one-dimensional insulator, see Fig. 5 (right) [46], resulting in an identical classification scheme.

The procedure is readily generalized to edges and corners of three-dimensional topological insulators. For the classification of edges of three-dimensional second-order topological insulators and superconductors, following Laughlin [42], we apply twisted periodic boundary conditions in the direction along the crystal edge with twist phases  $\varphi$ , effectively “rolling up” the crystal into a cylinder of finite thickness, see Fig. 6 (left). We again attach one-dimensional leads at each of the remaining sample edges, with the appropriate number of degrees of freedom  $g$ . Again, each lead is described by a unitary reflection matrix  $r_j$ , which now depends on the twist phase  $\varphi$ . Topologically protected gapless edge modes exist at the  $j$ th crystal edge if and only if the one-dimensional family of reflection matrices  $r_j(\varphi)$  is topologically nontrivial, where, as before, the precise definition of “topologically nontrivial” depends on the Altland-Zirnbauer class [43–45, 47]. For example, in class A, the winding number of  $\det r(\varphi)$  for  $0 < \varphi < 2\pi$  determines the integer topological index

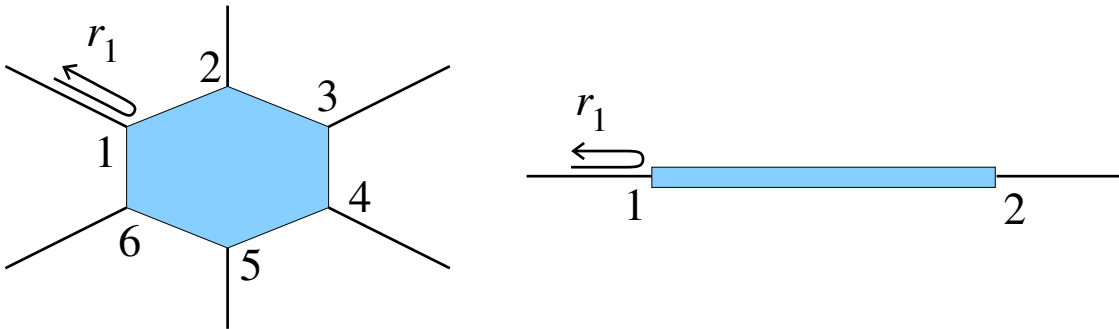


FIG. 5. Left: Two-dimensional second-order topological insulator (light blue), with one-dimensional leads attached to its corners. Right: One-dimensional topological insulator (light blue) with one-dimensional leads attached to its ends. In both cases each lead  $j$ , is described by a scattering matrix  $r_j$ .



[43], whereas in class AII the topological index is given by  $\text{Pf}[r(\pi)\sigma_2]\sqrt{\det r(0)}/\text{Pf}[r(0)\sigma_2]\sqrt{\det r(\pi)}$  [45, 47]. Again, the same argument can be applied to, and the same classification is obtained for the edge states of a standard two-dimensional topological insulator, see Fig. 6 (right).

We illustrate the procedure outlined above on a concrete example, the three-dimensional Hamiltonian (3) in class A in the main text. We consider a crystal infinite in the  $z$  direction, and with a cross section in the  $xy$  plane as in the inset of Fig. 7. We attach leads to all four vertical edges (corresponding to the four corners in the cross section of Fig. 7) and calculate the scattering matrix for electrons incident from these four leads. Translation invariance in the  $z$  direction allows us to fix the Bloch wavenumber  $k_z$ . We verify that there is no transmission between different leads, consistent with the fact that the bulk and the surfaces are gapped. Figure 7 shows that the total scattering phase  $\phi_j = \arg \det r_j(k_z)$  for the two leads attached to the edges carrying chiral edge state has non-zero winding number as a function of  $k_z$ , whereas there is no winding number for the leads attached to corners without topologically protected edge states.

## 2d SECOND-ORDER TIs WITHOUT CHIRAL AND PARTICLE-HOLE SYMMETRY

Inspection of our classification Table II shows that in 2d, the non-trivial second-order TIs are possible only in the presence of either chiral or particle-hole symmetry. This may seem to contradict the construction presented in Ref. 9, where a quantized quadrupole moment was predicted in the absence of these symmetries.

The resolution of the above contradiction lies in the fact that we require the edge-Hamiltonian (1d insulator) to be non-trivial TI (i.e. even in absence of any crystalline symmetries). We can relax this requirement and only demand that the edge-Hamiltonian is non-trivial TCI, thus when the two reflection symmetries are present, it is possible that a 1d edge-Hamiltonian is non-trivial TCI even in the absence of chiral and particle-hole symmetries [23, 24]. We note that in this scenario the existence of localized corner states is not guaranteed and one can only guarantee existence of the corner charges [51]. Another important difference is in the stability of the two above mentioned types of higher-order TIs, the ones described in the Table II require only *approximate* reflection symmetry as discussed in the main text, whereas in example of Ref. [9] the quadrupole quantization vanishes as soon as the reflection symmetry is broken.

## DISCUSSION OF THE REMAINING SYMMETRY CLASSES

Below we discuss the remaining symmetry classes for  $d = 2$  and  $d = 3$ . For higher dimensions ( $d > 3$ ) we use the isomorphisms between the corresponding  $K$ -groups [24] to obtain which reflection symmetry needs to be used, see Table II.

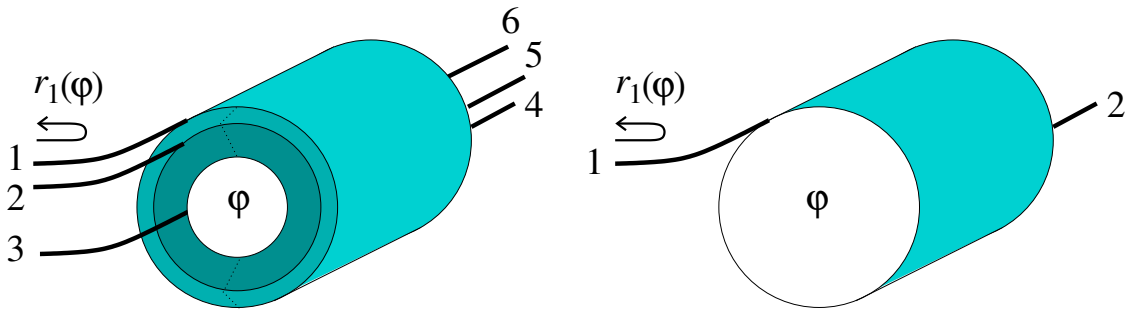


FIG. 6. Left: Three-dimensional second-order topological insulator (light blue), with one-dimensional leads attached to its edges. Right: Two-dimensional topological insulator (light blue) with one-dimensional leads attached to its edge. In both cases periodic boundary conditions with twist angle  $\varphi$  are applied in the direction of the edge. Each lead  $j$ , is described by a unitary scattering matrix  $r_j(\varphi)$ .

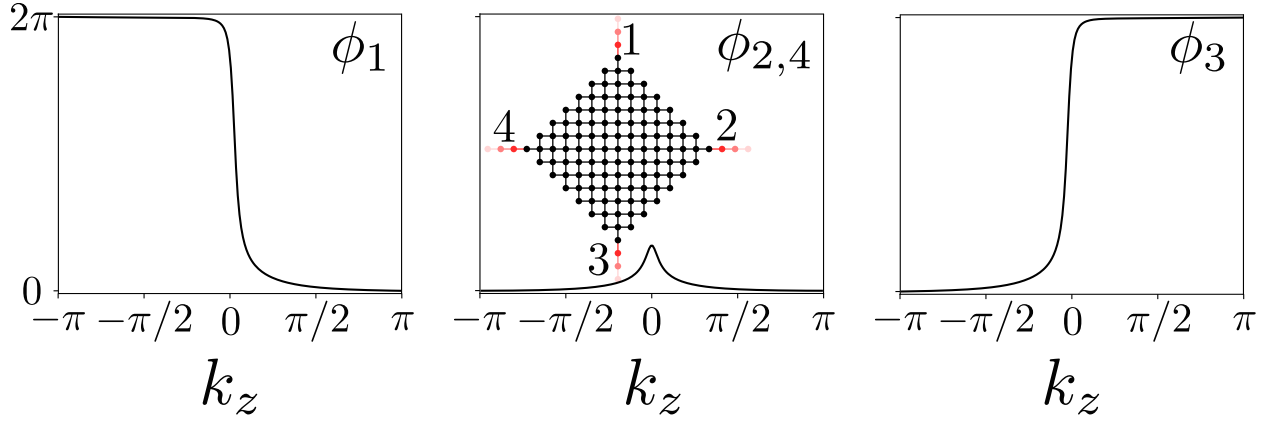


FIG. 7. The total scattering phase  $\phi_j = \arg \det r_j(k_z)$  of the reflection matrices  $r_j(k_z)$  for four leads  $j = 1, 2, 3, 4$  attached to the four vertical edges of the three-dimensional reflection-symmetric second-order topological insulator [Eq. (3) in the main text]. The inset shows a cross section in the  $xy$  plane indicating the position of the leads. Twisted periodic boundary conditions corresponding to the Bloch number  $k_z$  are applied in the  $z$  direction. The system size is  $30 \times 30$  sites and the parameters take the values  $m = 2$ ,  $B = 0.2$ . The scattering matrix is calculated at the energy  $\varepsilon = 0.1$ .

Cartan	$\mathcal{T}$	$\mathcal{P}$	$\mathcal{C}$	$d = 2$	$d = 3$	$d = 4$	$d = 5$	$d = 6$	$d = 7$	$d = 8$	$d = 9$
A	0	0	0	—	$\mathcal{R}(\mathbb{Z})$	—	$\mathcal{R}(\mathbb{Z})$	—	$\mathcal{R}(\mathbb{Z})$	—	$\mathcal{R}(\mathbb{Z})$
AIII	0	0	1	$\mathcal{R}_+(\mathbb{Z})$	—	$\mathcal{R}_+(\mathbb{Z})$	—	$\mathcal{R}_+(\mathbb{Z})$	—	$\mathcal{R}_+(\mathbb{Z})$	—
AI	1	0	0	—	—	—	$\mathcal{R}_+(\mathbb{Z})$ $\mathcal{R}_-(\mathbb{Z})$	—	$\mathcal{R}_+(\mathbb{Z}_2)$ $\mathcal{R}_-(\mathbb{Z}_2)$	$\mathcal{R}_+(\mathbb{Z}_2)$	$\mathcal{R}_+(\mathbb{Z})$
BDI	1	1	1	$\mathcal{R}_{++}(\mathbb{Z})$	—	—	—	$\mathcal{R}_{++}(\mathbb{Z})$ $\mathcal{R}_{--}(\mathbb{Z})$	—	$\mathcal{R}_{++}(\mathbb{Z}_2)$ $\mathcal{R}_{--}(\mathbb{Z}_2)$ $\mathcal{R}_{+-}$	$\mathcal{R}_{++}(\mathbb{Z}_2)$ $\mathcal{R}_{+-}$
D	0	1	0	$\mathcal{R}_+(\mathbb{Z}_2)$	$\mathcal{R}_+(\mathbb{Z})$	—	—	—	$\mathcal{R}_+(\mathbb{Z})$ $\mathcal{R}_-(\mathbb{Z})$	—	$\mathcal{R}_+(\mathbb{Z}_2)$ $\mathcal{R}_-(\mathbb{Z}_2)$
DIII	-1	1	1	$\mathcal{R}_{++}(\mathbb{Z})$ $\mathcal{R}_{--}(\mathbb{Z}_2)$ $\mathcal{R}_{-+}$	$\mathcal{R}_{++}(\mathbb{Z}_2)$ $\mathcal{R}_{-+}(\mathbb{Z}_2)$	$\mathcal{R}_{++}(\mathbb{Z})$	—	—	—	$\mathcal{R}_{++}(\mathbb{Z})$ $\mathcal{R}_{--}(\mathbb{Z})$	—
AII	-1	0	0	—	$\mathcal{R}_+(\mathbb{Z}_2)$ $\mathcal{R}_-(\mathbb{Z}_2)$	$\mathcal{R}_+(\mathbb{Z}_2)$	$\mathcal{R}_+(\mathbb{Z})$	—	—	—	$\mathcal{R}_+(\mathbb{Z})$ $\mathcal{R}_-(\mathbb{Z})$
CII	-1	-1	1	$\mathcal{R}_{++}(\mathbb{Z})$ $\mathcal{R}_{--}(\mathbb{Z})$	—	$\mathcal{R}_{++}(\mathbb{Z}_2)$ $\mathcal{R}_{--}(\mathbb{Z}_2)$ $\mathcal{R}_{+-}$	$\mathcal{R}_{++}(\mathbb{Z}_2)$ $\mathcal{R}_{+-}(\mathbb{Z}_2)$	$\mathcal{R}_{++}(\mathbb{Z})$	—	—	—
C	0	-1	0	—	$\mathcal{R}_+(\mathbb{Z})$ $\mathcal{R}_-(\mathbb{Z})$	—	$\mathcal{R}_+(\mathbb{Z}_2)$ $\mathcal{R}_-(\mathbb{Z}_2)$	$\mathcal{R}_+(\mathbb{Z}_2)$	$\mathcal{R}_+(\mathbb{Z})$	—	—
CI	1	-1	1	—	—	$\mathcal{R}_{++}(\mathbb{Z})$ $\mathcal{R}_{--}(\mathbb{Z})$	—	$\mathcal{R}_{++}(\mathbb{Z}_2)$ $\mathcal{R}_{--}(\mathbb{Z}_2)$ $\mathcal{R}_{-+}$	$\mathcal{R}_{++}(\mathbb{Z}_2)$ $\mathcal{R}_{-+}(\mathbb{Z}_2)$	$\mathcal{R}_{++}(\mathbb{Z})$	—

TABLE II. Extension of Tab. I in the main text including higher dimensions.

$$d = 2$$

Below we discuss for each of the nontrivial reflection-symmetric Altland-Zirnbauer classes whether there are second-order topological insulators if two of the faces are related by reflection symmetry. The ten Altland-Zirnbauer classes are defined through the presence or absence of time reversal symmetry  $\mathcal{T}$ , particle-hole symmetry  $\mathcal{P}$ , and chiral symmetry  $\mathcal{C}$ , distinguishing the cases  $\mathcal{T}^2 = \pm 1$  and  $\mathcal{P}^2 = \pm 1$ . Explicitly, the three symmetry operations read

$$H(\mathbf{k}) = U_{\mathcal{T}} H(-\mathbf{k})^* U_{\mathcal{T}}^\dagger, \quad (6)$$

$$H(\mathbf{k}) = -U_{\mathcal{P}} H(-\mathbf{k})^* U_{\mathcal{P}}^\dagger, \quad (7)$$

$$H(\mathbf{k}) = -U_{\mathcal{C}} H(\mathbf{k}) U_{\mathcal{C}}^\dagger, \quad (8)$$



where  $U_{\mathcal{T}}$ ,  $U_{\mathcal{P}}$ , and  $U_{\mathcal{C}}$  are unitary matrices with  $U_{\mathcal{T}}U_{\mathcal{T}}^* = \mathcal{T}^2$  and  $U_{\mathcal{P}}U_{\mathcal{P}}^* = \mathcal{P}^2$ . If  $\mathcal{T}$  and  $\mathcal{P}$  are both present, one has  $U_{\mathcal{C}} = U_{\mathcal{T}}U_{\mathcal{P}}^*$ .

Reflection symmetry gives one more symmetry relation for  $H$ ,

$$H(\mathbf{k}) = U_{\mathcal{R}}H(R\mathbf{k})U_{\mathcal{R}}^\dagger, \quad (9)$$

where  $R\mathbf{k} = (-k_1, k_2)$  in two dimensions and  $R\mathbf{k} = (-k_1, k_2, k_3)$  in three dimensions. The unitary matrix  $U_{\mathcal{R}}$  is chosen such that the reflection operation has the appropriate commutation or anticommutation relations with the  $\mathcal{T}$  and  $\mathcal{P}$  operations. The precise choices for the unitary matrices  $U_{\mathcal{T}}$ ,  $U_{\mathcal{P}}$ ,  $U_{\mathcal{C}}$ , and  $U_{\mathcal{R}}$  depend on the symmetry class under consideration and will be specified for each symmetry class separately. Since the group structure follows from the general classification procedure of second-order topological insulators and superconductors, it is sufficient to show that the reflection-symmetric models provide the generators.

### Class AIII

*With reflection symmetry  $\mathcal{R}_+$ .*—Class AIII has chiral symmetry only, which we represent using  $U_{\mathcal{C}} = \sigma_3$ . We represent the reflection symmetry using  $U_{\mathcal{R}} = \sigma_3\tau_3$ . This class has a  $\mathbb{Z}$  topological index, which counts the difference between the number of helical edge states with positive and negative eigenvalue of  $\tau_3$ . A “minimal” edge, which will serve as a generator for the corresponding class of second-order TIs, has a single helical state with (say) a positive eigenvalue of  $\tau_3$ , so that the reflection operation for edge states is effectively represented by  $U_{\mathcal{R},\text{edge}} = \sigma_3$  and the edge Hamiltonian is

$$H_{\text{edge}} = v(\sigma_1 \cos \varphi + \sigma_2 \sin \varphi)k_1. \quad (10)$$

In the absence of reflection symmetry, such an edge Hamiltonian has the unique mass term  $m(\sigma_1 \sin \varphi - \sigma_2 \cos \varphi)$ , which is *odd* under reflection. Hence, the intersection of two reflection-related edges corresponds to a domain wall for the edge theory, which harbors a localized state at zero energy.

### Class BDI

*With reflection symmetry  $\mathcal{R}_{++}$ .*—Class BDI has time-reversal symmetry and particle hole symmetry with  $\mathcal{T}^2 = \mathcal{P}^2 = 1$ . We here represent time-reversal symmetry by complex conjugation  $K$  and particle-hole symmetry by  $\tau_3K$ , so that the two-dimensional Hamiltonian satisfies

$$\begin{aligned} H(k_1, k_2) &= H(-k_1, -k_2)^* \\ &= -\tau_3 H(k_1, k_2) \tau_3. \end{aligned} \quad (11)$$

A reflection symmetry commuting with  $\mathcal{T}$  and  $\mathcal{P}$  can be represented by  $U_{\mathcal{R}} = \tau_3\sigma_3$ , leading to the additional constraint  $H(k_1, k_2) = \tau_3\sigma_3H(-k_1, k_2)\sigma_3\tau_3$ . Class BDI with  $\mathcal{R}_{++}$  reflection symmetry has a  $\mathbb{Z}$  classification. The integer invariant counts the difference of the number of helical edge states with positive and negative eigenvalues of  $\tau_3$ . The minimal reflection-symmetric nontrivial edge has a single helical state with (say) positive eigenvalue of  $\tau_3$ , so that effectively for the edge one reflection is represented by  $\sigma_3$ . The corresponding minimal edge Hamiltonian is  $H_{\text{edge}} = vk_1\sigma_2$  and the unique mass term opening a gap in  $H_{\text{edge}}$  is  $m\sigma_1$ , which is odd under reflection.

### Class D

*With reflection symmetry  $\mathcal{R}_+$ .*—We refer to the discussion in the main text.

### Class DIII

For Altland-Zirnbauer class DIII we choose the representations  $U_{\mathcal{T}} = \sigma_2$ ,  $U_{\mathcal{P}} = 1$ , so that

$$\begin{aligned} H(k_1, k_2) &= -H(-k_1, -k_2)^* \\ &= -\sigma_2 H(k_1, k_2) \sigma_2. \end{aligned} \quad (12)$$

This symmetry class has a  $\mathbb{Z}_2$  topological invariant in two dimensions, which counts the parity of the number of helical Majorana edge modes. A single helical Majorana edge mode has Hamiltonian

$$H_1 = vk_1\sigma_3 \quad (13)$$

and can not be gapped out by any perturbation that preserves time-reversal and particle-hole symmetry. A pair of Majorana modes, however, with edge Hamiltonian

$$H_2 = vk_1\sigma_3\tau_0, \quad (14)$$

can be gapped out by the unique mass term  $m\sigma_1\tau_2$ . As in the case of class AIII discussed above, the choice for the edge Hamiltonians  $H_1$  and  $H_2$  is not unique, but different choices are related by an orthogonal transformation, and the same orthogonal transformation needs to be applied to the otherwise unique mass term.

*With reflection symmetry  $\mathcal{R}_{++}$ .*—We represent a reflection operation that commutes with  $\mathcal{T}$  and  $\mathcal{P}$  by  $U_{\mathcal{R}} = \tau_2\sigma_2$ . The corresponding topological classification is  $\mathbb{Z}_2$ . The reflection symmetry is incompatible with the existence of only a single helical Majorana mode. The mass term  $m\sigma_1\tau_2$  for a pair of Majorana modes is odd under reflection operation, so that the generator of DIII $^{\mathcal{R}_{++}}$  also serves as a generator for the corresponding class of second-order topological superconductors. [Note that a quartet of helical states, with edge Hamiltonian  $H_4 = vk\sigma_3\tau_0\rho_0$ , can be gapped out, using the reflection-symmetric mass terms  $m\sigma_1\tau_1\rho_2$  or  $m\sigma_1\tau_3\rho_2$ , consistent with the  $\mathbb{Z}_2$  index for this symmetry class.]

*With reflection symmetry  $\mathcal{R}_{--}$ .*—We represent a reflection operation that anticommutes with  $\mathcal{T}$  and  $\mathcal{P}$  by  $U_{\mathcal{R}} = \tau_3\sigma_2$ . With this reflection symmetry there is a  $\mathbb{Z}$  topological invariant, which counts the difference of the number of helical edge states with positive and negative eigenvalues of  $\tau_3$ . For a “minimal” edge all  $\tau_3$ -eigenvalues are (say) positive and one may effectively use the representation  $U_{\mathcal{R}} = \sigma_2$ . Indeed, the combination of reflection symmetry, particle-hole symmetry, and time-reversal symmetry then forbids any mass term that would gap out helical edge modes. Only topological crystalline phases with an even number of helical modes can be used for the construction of a second-order topological insulator, since a single helical Majorana mode corresponds to a strong topological phase. Each pair of helical modes leads to a Majorana-Kramers pair at the intersection between reflection-related edges. A pair of Majorana-Kramers pairs is unstable, however, to a local perturbation at the sample corner and can be gapped out without closing the bulk and edge gaps.

*With reflection symmetry  $\mathcal{R}_{-+}$ .*—In this case we take  $U_{\mathcal{R}} = \tau_3\sigma_1$ . The corresponding  $\mathbb{Z}_2^2$  classification counts the parity of the number of helical Majorana modes for each  $\tau_3$ -eigenvalue. Topological phases with an odd number of helical Majorana modes are topologically nontrivial already in the absence of reflection symmetry and cannot be used for the construction of a second-order topological superconductor. Since a pair of helical Majorana modes with the same  $\tau_3$ -eigenvalue can be gapped out by the reflection-symmetric mass term  $\sigma_1\rho_2$ , the relevant topological crystalline phase has a pair of helical Majorana modes with different  $\tau_3$ -eigenvalues: In this case the edge modes are protected by reflection symmetry, since the reflection symmetry forbids the unique mass term  $m\sigma_1\tau_2$ .

### Class CII

Altland-Zirnbauer class CII has  $\mathcal{T}^2 = \mathcal{P}^2 = -1$ , which is implemented by choosing  $U_{\mathcal{T}} = \sigma_2$  and  $U_{\mathcal{P}} = \sigma_2\tau_3$ , so that  $H(k_1, k_2)$  satisfies the symmetry constraints

$$\begin{aligned} H(k_1, k_2) &= \sigma_2 H(-k_1, -k_2)^* \sigma_2 \\ &= -\tau_3 H(k_1, k_2) \tau_3. \end{aligned} \quad (15)$$

*With reflection symmetry  $\mathcal{R}_{++}$ .*—We represent the reflection symmetry by  $U_{\mathcal{R}} = \tau_3\rho_3$ . The corresponding symmetry class has a  $2\mathbb{Z}$  classification, see Refs. [21, 23, 52], which counts difference of “edge quartets” with positive and negative eigenvalue of  $\rho_3$ . The minimal nontrivial edge has a single quartet with positive eigenvalue of  $\rho_3$ , so that effectively  $\mathcal{R}$  is represented by  $\tau_3$ . The corresponding edge Hamiltonian has the form

$$H_{\text{edge}} = ivk \begin{pmatrix} 1 & 0 \\ 0 & n \end{pmatrix} \begin{pmatrix} 0 & i \\ -i & 0 \end{pmatrix} \begin{pmatrix} 1 & 0 \\ 0 & n^\dagger \end{pmatrix} \quad (16)$$

where  $n$  is a (real) quaternion of unit modulus,  $n = n_0 + i \sum_{j=1}^3 n_j \sigma_j$ , with  $\sum_{j=0}^3 n_j^2 = 1$ . The unique mass term gapping out  $H_{\text{edge}}$  is

$$m \begin{pmatrix} 1 & 0 \\ 0 & n \end{pmatrix} \begin{pmatrix} 0 & 1 \\ 1 & 0 \end{pmatrix} \begin{pmatrix} 1 & 0 \\ 0 & n^\dagger \end{pmatrix},$$

and is odd under reflection. [Note that no mass terms can be added as long as all edge quartets have the same  $\rho_3$  eigenvalue, consistent with the  $2\mathbb{Z}$  topological index for this class.]

*With reflection symmetry  $\mathcal{R}_{--}$ .*—Proceeding as in the previous case, we represent  $\mathcal{R}$  by  $\sigma_3$ . For the helical edge we choose the reflection-symmetric edge Hamiltonian

$$H_{\text{edge}} = vk_1(\sigma_1 \cos \varphi + \sigma_2 \sin \varphi)\tau_1, \quad (17)$$

and note that the unique mass term  $m(\sigma_1 \sin \varphi - \sigma_2 \cos \varphi)\tau_2$  is odd under reflection. (Note that upon doubling the number of edge states, *e.g.*, taking  $H_{\text{edge}} = vk_1\sigma_2\tau_1\rho_0$ , a reflection-symmetric mass term  $\tau_2\rho_2$  exists, consistent with the  $\mathbb{Z}_2$  topological index for this class [23, 52].)

$$d = 3$$

We close with a discussion of the nontrivial reflection-symmetric Altland-Zirnbauer classes in three dimensions, which become second-order topological insulators if two of the faces are related by reflection symmetry.

#### Class A

*With reflection symmetry  $\mathcal{R}$ .*—We refer to the main text for a discussion.

#### Class D

*With reflection symmetry  $\mathcal{R}_+$ .*—As in the two dimensional case, we represent particle-hole conjugation by complex conjugation and reflection by  $U_{\mathcal{R}} = \sigma_1$ , so that  $H(k_1, k_2, k_3)$  satisfies

$$\begin{aligned} H(k_1, k_2, k_3) &= -H(-k_1, -k_2, -k_3)^* \\ &= \sigma_1 H(-k_1, k_2, k_3) \sigma_1. \end{aligned} \quad (18)$$

The corresponding symmetry class has a  $\mathbb{Z}$  classification. A generator has surface Hamiltonian

$$H_{\text{surface}} = v(k_1\sigma_3 + k_2\sigma_1), \quad (19)$$

where we choose the (001) surface as a prototype for a reflection-symmetric surface. The unique mass term gapping out these surface states is  $m\sigma_2$ , which is odd under reflection. The intersection of two surfaces related by reflection symmetry corresponds to a domain wall in the effective surface theory, which hosts a chiral Majorana mode [15].

#### Class DIII

We again choose the representations  $U_{\mathcal{T}} = \sigma_2$ ,  $U_{\mathcal{P}} = 1$ , so that

$$\begin{aligned} H(k_1, k_2, k_3) &= -H(-k_1, -k_2, -k_3)^* \\ &= -\sigma_2 H(k_1, k_2, k_3) \sigma_2. \end{aligned} \quad (20)$$

This symmetry class has a  $\mathbb{Z}$  topological invariant in three dimensions, which counts the number of Majorana Dirac cones at the surface. A single Majorana Dirac cone has Hamiltonian

$$H_2 = v(k_1\sigma_1 + k_2\sigma_3) \quad (21)$$

and can not be gapped out by any perturbation that preserves time-reversal and particle-hole symmetry. The same applies to multiple Dirac cones described by the Hamiltonian (21), as long as they have the same chirality (which is well defined because terms proportional to  $\sigma_2$  are forbidden by the chiral symmetry).

*With reflection symmetry  $\mathcal{R}_{++}$ .*—We represent the reflection operation by  $U_{\mathcal{R}} = \tau_1$ . A single Majorana Dirac cone is incompatible with reflection symmetry. A pair of Dirac cones with opposite chirality is allowed under reflection, however, with surface Hamiltonian

$$H_2 = v(k_1\sigma_1\tau_3 + k_2\sigma_3\tau_0). \quad (22)$$

Such a pair can be gapped out by the unique mass term  $m\tau_2\sigma_1$ , which is odd under reflection. [Note that upon doubling the number of Majorana Dirac cones, setting  $H_2 = v(k_1\sigma_1\tau_3 + k_2\sigma_3\tau_0)\rho_0$  the mass term  $m = \rho_2\sigma_1$  is allowed under reflection symmetry, consistent with the  $\mathbb{Z}_2$  topological classification for this symmetry class.]

*With reflection symmetry  $\mathcal{R}_{-+}$ .*—This reflection symmetry can be represented by the Pauli matrix  $U_{\mathcal{R}} = \sigma_3$ . This symmetry class has a  $\mathbb{Z}^2$  topological classification, where the integer invariants count the number of Majorana Dirac cones of each chirality. As in the previous example, a single pair of Majorana Dirac cones with opposite chirality can be gapped out by the mass term  $m\tau_2\sigma_1$ , which is odd under reflection. [Note that, although this symmetry class allows for multiple Majorana Dirac cones, an even number of helical Majorana modes at the intersection of two reflection-related surfaces is unstable to local perturbations at the edge.]

*With reflection symmetry  $\mathcal{R}_{+-}$ .*—Although the reflection symmetry  $\mathcal{R}_{+-}$  allows for a nontrivial topological phase, these are the same phases as in the absence of reflection symmetry, so that this symmetry class can not be used to construct a second-order topological superconductor. To see this explicitly, we choose the representation  $U_{\mathcal{R}} = \tau_2\sigma_3$ . One then verifies that the reflection symmetry is compatible with an integer number of pairs of Majorana Dirac cones of the same chirality, described by the surface Hamiltonian

$$H_{2\pm} = v(\pm k_1\sigma_1 + k_2\sigma_3)\tau_0. \quad (23)$$

The  $\mathbb{Z}$  topological invariant counts the difference of such Majorana Dirac pairs of positive and negative parity. The nontrivial topological realizations are also nontrivial without reflection symmetry, *i.e.*, they are a strong topological phase.

### Class AII

*With reflection symmetry  $\mathcal{R}_-$ .*—See the discussion in the main text.

*With reflection symmetry  $\mathcal{R}_+$ .*—We choose the representation  $U_{\mathcal{T}} = \sigma_2$  and  $U_{\mathcal{R}} = \sigma_1\tau_2$ , for which a pair of surface Dirac cones, described by the Hamiltonian

$$H_2 = v(k_1\sigma_2 + k_2\sigma_1)\tau_0, \quad (24)$$

is gapped out by a unique mass term  $m\sigma_3\tau_2$ , which is odd under reflection. [A quartet of surface Dirac cones can be gapped out in the presence of reflection symmetry, however, consistent with the  $\mathbb{Z}_2$  topological index for this symmetry class.]

### Class C

This symmetry class has particle-hole symmetry squaring to  $-1$ , which is represented by  $\sigma_2K$ . Hamiltonians in this symmetry class then satisfy the symmetry constraint

$$H(k_1, k_2, k_3) = -\sigma_2 H(-k_1, -k_2, -k_3)^* \sigma_2. \quad (25)$$

*With reflection symmetry  $\mathcal{R}_+$ .*—We choose to represent reflection by  $U_{\mathcal{R}} = \tau_3$  and consider a pair of surface Andreev Dirac cones with Hamiltonian

$$H_2 = v(k_1\tau_1 + k_2\tau_3)\sigma_0 \quad (26)$$

This surface Hamiltonian is gapped out by the unique mass term  $m\sigma_0\tau_2$ , which is odd under reflection. The intersection of two reflection-related surfaces then has a domain wall in the effective surface theory, which gives a chiral Andreev mode at the corresponding crystal edge. [Note that multiple surface Majorana Dirac cones with Hamiltonian (26) are protected in the presence of reflection symmetry, consistent with the  $2\mathbb{Z}$  topological index for this symmetry class.]

*With reflection symmetry  $\mathcal{R}_-$ .* We represent the anticommuting reflection operation by  $U_{\mathcal{R}} = \sigma_1\tau_3$ . This symmetry class has a  $\mathbb{Z}_2$  topological index. The anticommuting reflection symmetry is compatible with a pair of surface Andreev Dirac cones with Hamiltonian (26), and the mass term  $m\sigma_0\tau_2$  remains odd under reflection. Consistent with the  $\mathbb{Z}_2$  topological index, a quartet of Andreev Dirac cones with Hamiltonian  $H_2 = v(k_1\tau_1 + k_2\tau_3)\sigma_0\rho_0$  can be gapped out by a reflection-allowed mass term  $m\tau_2\sigma_2\rho_2$ .

---